

Li⁺, Na⁺, and K⁺ Binding to the DNA and RNA Nucleobases. Bond Energies and Attachment Sites from the Dissociation of Metal Ion-Bound Heterodimers

Blas A. Cerda and Chrys Wesdemiotis*

Contribution from the Department of Chemistry, The University of Akron, Akron, Ohio 44325-3601

Received April 23, 1996[⊗]

Abstract: The alkali metal ion ($M^+ = \text{Li}^+, \text{Na}^+, \text{K}^+$) affinities of the common DNA and RNA nucleobases are determined in the gas phase by investigating the dissociation of metal ion-bound heterodimers [nucleobase + B] M^+ , in which B represents a reference base of known affinity (kinetic method). The dimer ion decompositions are assessed at two different internal energies, namely from metastable precursor ions and after collisional activation. This approach makes it possible to deconvolute entropy from enthalpy and, therefore, leads to more accurate affinity (i.e. enthalpy or bond energy) values. For the nucleobases studied, viz. guanine, cytosine, adenine, thymine, and uracil, the corresponding M^+ -nucleobase bond energies are (kJ mol⁻¹) as follows: 239, 232, 226, 215, and 211 with Li⁺; 182, 177, 172, 144, and 141 with Na⁺; and 117, 110, 106, 102, and 101 with K⁺. The method used also provides quantitative information about the overall entropy change occurring upon the dissociation of the heterodimers; this change is most significant when dissociation alters rotational degrees of freedom. The magnitude of the operating entropy effects gives information on the structures of both the metal ion-bound dimers and the metalated nucleobase monomers. It is found that Li⁺, Na⁺, and K⁺ bind very similarly to the nucleobases. Attachment sites that explain the observed entropic effects and metal ion affinity orders are suggested and discussed. A notable characteristic of several of the resulting structures is their ability to form stabilizing ion pairs (salt bridges).

Introduction

The free and protein-bound forms of the alkali metal ions Li⁺, Na⁺, and K⁺ are significant participants in several processes of nucleic acid metabolism. Synthesis, replication, and cleavage of DNA and RNA as well as their structural integrity are affected by the presence of these ionized metals in the cell nucleus. At low concentration, the alkali metal ions interact with the negatively charged phosphate groups of the nucleic acid chain to provide a stabilizing effect through charge neutralization. At higher concentration, the metal ions may interact with the nucleobases and disrupt base pair hydrogen bonding, compromising this way the structural integrity of the nucleic acid polymer.^{1,2} Additionally, the alkali metal ions have an inhibitory effect on the chain initiation process by RNA polymerases which may in turn alter the extent and fidelity of RNA synthesis.²

Whether and where a specific alkali metal ion will interact with a nucleic acid is controlled, at least in part, by the relative bond strength between the metal ion and the possible donor groups present in the nucleic acid chain. Knowledge about the fundamental modes of metal ion binding to simple DNA and RNA components (nucleobases, nucleosides, etc.) would greatly improve our understanding on how metal ions interact with more complex nucleic acid structures. The present study addresses this topic by assessing the Li⁺, Na⁺, and K⁺ affinities of the DNA and RNA nucleobases guanine (G), cytosine (C), adenine (A), thymine (T), and uracil (U) by tandem mass spectrometry (MS/MS).³ The diluted gas phase of the mass spectrometer

provides an ideal medium to establish these important intrinsic properties without complicating or interfering solvent effects.

In spite of the important role that mass spectral methods have played in elucidating the metal ion chemistry of biomolecules, relatively few studies so far have focused on the complexes of Li⁺, Na⁺, and K⁺ with nucleic acid constituents.^{4–12} Moreover, the majority of published work has not concerned the M^+ adducts of nucleobases but those of larger units, such as nucleosides and nucleotides. More than 10 years ago, it was recognized that the Na⁺ attachment ions of oligonucleotides are readily generated by fast atom bombardment (FAB) or laser desorption (LD) and that the so produced precursor ions can yield sequence diagnostic fragments.^{4,5} Gross et al. reported that the mass spectra of alkali ion cationized nucleosides include prominent ions in which the metal ion is affiliated with the nucleobase (NB).^{5,6} Later work by Voyksner showed that the intensity of [nucleotide + M]⁺ increases as the radius of the alkali metal ion decreases.⁸ In a newer study, Madhusudanan et al. presented the MS/MS spectra of [dinucleotide + Li]⁺ cations, in which the relative abundance of the [NB]Li⁺ peaks

(3) Busch, K. L.; Glish, G. L.; McLuckey, S. A. *Mass Spectrometry/Mass Spectrometry*; VCH Publishers: New York, 1988.

(4) Aubagnac, J. L.; Devienne, T. M.; Combarieu, R.; Barascut, J. L.; Imbach, J. L.; Lazrek, H. B. *Org. Mass Spectrom.* **1983**, *18*, 361–364.

(5) McCreery, D. A.; Gross, M. L. *Anal. Chim. Acta* **1985**, *178*, 91–103.

(6) Tomer, K. B.; Gross, M. L. *Anal. Chem.* **1986**, *58*, 2527–2534.

(7) Hogg, A. M.; Kelland, J. G.; Vederas, C. J. *Helv. Chim. Acta* **1986**, *69*, 908–917.

(8) Voyksner, R. D. *Org. Mass Spectrom.* **1987**, *22*, 513–518.

(9) Chiarelli, M. P.; Gross, M. L. *J. Phys. Chem.* **1989**, *93*, 3595–3599.

(10) Madhusudanan, K. P.; Katti, S. B.; Hashmi, S. A. N. *Org. Mass Spectrom.* **1993**, *28*, 970–976.

(11) Paul, G. J. C.; Theophanides, T.; Anastassopoulou, J.; Marcotte, I.; Bertrand, M. *Proceedings of the 43rd ASMS Conference on Mass Spectrometry and Allied Topics*; May 21–26, 1995, Atlanta, GA; p 608.

(12) Rodgers, M. T.; Armentrout, P. B. *Proceedings of the 44th ASMS Conference on Mass Spectrometry and Allied Topics*; May 12–16, 1996, Portland, OR; p 88.

[⊗] Abstract published in *Advance ACS Abstracts*, November 15, 1996.

(1) (a) Lippard, S. J.; Berg, J. M. *Principles of Bioinorganic Chemistry*; University Science Books: Mill Valley, CA, 1994. (b) Kaim, W.; Schwedersky, B. *Bioinorganic Chemistry: Inorganic Elements in the Chemistry of Life*; John Wiley & Sons: Chichester, 1994.

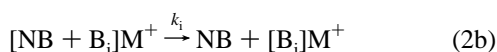
(2) Loeb, L. A.; Zakour, A. R. In *Nucleic Acid–Metal Ion Interactions*; Spiro, T. G., Ed.; John Wiley & Sons: New York, 1980; pp 115–144.

rose in the order T ≪ A < C < G,¹⁰ presumably because of increasing nucleobase basicity in this direction.¹³ The observation of [NB]M⁺ ions from larger precursors (which also contain sugar and phosphate residues) points out that the nucleobases can offer competitive coordination sites to the metal ion. This study identifies the likely location of these sites, based on the order of affinities derived and the entropy effects observed upon dissociation of M⁺-bound heterodimers of the nucleobases. A parallel investigation on the binding of M⁺ to nucleobases, employing guided ion beam mass spectrometry, has recently been reported by Rodgers and Armentrout.¹²



The alkali metal ion affinity of a nucleobase is defined as the enthalpy change of reaction 1 and corresponds to the dissociation energy of the NB–M⁺ bond. Metal ion–ligand bond energies can be ascertained by several methods,^{14,15} *inter alia* guided ion beam experiments involving endothermic reactions,¹⁶ equilibrium and bracketing approaches,¹⁷ photodissociation,¹⁸ analysis of the kinetic energy release distributions resulting upon decomposition,¹⁹ and from the kinetics of dissociation of metal ion bound dimers (kinetic method).^{20–23} The latter technique, developed by Cooks and co-workers,²⁴ is employed here in a modified version as described in the following section. A closely related procedure was used by Fenselau et al. in the determination of proton affinities.²⁵

Dissociation of Metal Ion-Bound Dimers at Different Internal Energies. The kinetic method compares the rates of dissociation of a M⁺-bound dimer to each of the individual metalated monomers to estimate the difference in metal ion affinities between the two monomers. For heterodimers between a nucleobase, NB, and a series of reference bases, B_i, the relevant dissociations are:



Using transition state theory,²⁶ the ratio of the corresponding rate constants is given by eq 3, where Q^* and Q_i^* are the partition functions of the activated complexes for reaction 2a

(13) For the proton affinities of the DNA nucleobases see: (a) Greco, F.; Liguori, A.; Sindona, G.; Uccella, N. *J. Am. Chem. Soc.* **1990**, *112*, 9092–9096. (b) Rodgers, M. T.; Campbell, S.; Marzluff, M.; Beauchamp, J. L. *Int. J. Mass Spectrom. Ion Processes* **1995**, *148*, 1–23.

(14) Martinho Simões, J. A.; Beauchamp, J. L. *Chem. Rev.* **1990**, *90*, 629–688.

(15) Eller, K.; Schwarz, H. *Chem. Rev.* **1991**, *91*, 1121–1177.

(16) Armentrout, P. B. In *Gas Phase Inorganic Chemistry*; Russell, D. H., Ed.; Plenum Press: New York, 1989; pp 1–42.

(17) Uppal, K.; Lebrilla, C. B.; Drewello, T.; Schwarz, H. *J. Am. Chem. Soc.* **1988**, *110*, 3068–3071.

(18) Cassady, C. J.; Freiser, B. S. *J. Am. Chem. Soc.* **1984**, *106*, 6176–6179.

(19) Van Koppen, P. A. M.; Jacobson, D. B.; Illies, A.; Bowers, M. T.; Hanratty, M.; Beauchamp, J. L. *J. Am. Chem. Soc.* **1989**, *111*, 1991–2001.

(20) Chen, L.-Z.; Miller, J. M. *J. Am. Soc. Mass Spectrom.* **1991**, *2*, 120–124.

(21) Bojesen, G.; Breindahl, T.; Andersen, U. *Org. Mass Spectrom.* **1993**, *28*, 1448–1452.

(22) Cerda, B. A.; Wesdemiotis, C. *J. Am. Chem. Soc.* **1995**, *117*, 9734–9739.

(23) Cooks, R. G.; Patrick, J. S.; Kotiaho, T.; McLuckey, S. A. *Mass Spectrom. Rev.* **1994**, *13*, 287–339.

(24) McLuckey, S. A.; Cameron, D.; Cooks, R. G. *J. Am. Chem. Soc.* **1981**, *103*, 1313–1317.

(25) Cheng, X.; Wu, Z.; Fenselau, C. *J. Am. Chem. Soc.* **1993**, *115*, 4844–4848.

(26) Robinson, P. J.; Holbrook, K. A. *Unimolecular Reactions*; Wiley-Interscience: London, 1972.

or 2b, respectively, ϵ° and ϵ_i° are the corresponding activation energies, and T_{eff} is the effective temperature of the dissociating dimer ion $[\text{NB} + \text{B}_i]\text{M}^+$. If the reverse activation energies of fragmentations 2a and 2b are negligible (which is corroborated by their small kinetic energy releases),^{27,28} $\epsilon_i^{\circ} - \epsilon^{\circ}$ can be approximated by $\Delta H_{\text{M}^+}^{\circ}(\text{NB}) - \Delta H_{\text{M}^+}^{\circ}(\text{B}_i) = \Delta(\Delta H_{\text{M}^+}^{\circ})$, i.e. by the relative metal ion affinity of the two bases comprising the metal ion-bound dimer (eq 4).

$$\ln(k/k_i) = \ln(Q^*/Q_i^*) + (\epsilon_i^{\circ} - \epsilon^{\circ})/RT_{\text{eff}} \quad (3)$$

$$\ln(k/k_i) = \ln(Q^*/Q_i^*) + \Delta(\Delta H_{\text{M}^+}^{\circ})/RT_{\text{eff}} \quad (4)$$

In such a case, the term $\ln(Q^*/Q_i^*)$ is equal to the difference in entropy change between reactions 2a and 2b, viz. $-\Delta(\Delta S_{\text{M}^+}^{\circ})$.^{23–26} Substitution of $\ln(Q^*/Q_i^*)$ by $-\Delta(\Delta S_{\text{M}^+}^{\circ})/R$ leads to eq 5,

$$\ln(k/k_i) = -\Delta(\Delta S_{\text{M}^+}^{\circ})/R + \Delta(\Delta H_{\text{M}^+}^{\circ})/RT_{\text{eff}} = \Delta(\Delta G_{\text{M}^+}^{\circ})/RT_{\text{eff}} \quad (5)$$

from which it is evident that the kinetic measurement provides free energies, not enthalpies, unless there are justifiable reasons to neglect the entropic parameter. If $\Delta(\Delta S_{\text{M}^+}^{\circ}) \approx 0$ (i.e. if $Q^* \approx Q_i^*$), which usually holds when NB and B_i are structurally similar compounds forming the same type of bond(s) to M⁺, eqs 4 and 5 further simplify to

$$\ln(k/k_i) = \Delta H_{\text{M}^+}^{\circ}(\text{NB})/RT_{\text{eff}} - \Delta H_{\text{M}^+}^{\circ}(\text{B}_i)/RT_{\text{eff}} \quad (6)$$

directly relating the difference in alkali ion affinities of the bases being compared to the experimentally measurable rate constant ratio; the latter is equal to the ratio of the abundances of $[\text{NB}]\text{M}^+$ and $[\text{B}_i]\text{M}^+$ in the MS/MS spectrum of $[\text{NB} + \text{B}_i]\text{M}^+$. With a series of reference bases B_i, a plot of $\ln(k/k_i)$ versus $\Delta H_{\text{M}^+}^{\circ}(\text{B}_i)$ supplies the effective temperature and the desired $\Delta H_{\text{M}^+}^{\circ}(\text{NB})$ value.

Owing to its underlying assumptions, the relationship of eq 6 is best applied to ionic heterodimers of chemically and structurally similar species that undergo simple dissociations. Granted these prerequisites, eq 6 can successfully be used to estimate various types of bond energies, e.g., proton affinities, gas-phase acidities, metal and chloride ion affinities, and electron affinities.²³ The kinetic method has provided relative proton affinities of amino acids and small peptides^{29,30} that are in very good agreement with values measured by more accurate equilibrium or bracketing approaches.^{30,31} It has been of particular value for polar biomolecules, which are difficult to study by other techniques because they cannot be vaporized without degradation and/or are not available in pure form. This capability was recently demonstrated in our laboratory by the determination of the relative Cu(I) affinities of 18 mammalian amino acids, including thermally labile cysteine, glutamine, and histidine.²² Discrepancies have however been documented, indicating that in certain cases entropic effects cannot be

(27) Cooks, R. G.; Beynon, J. H.; Caprioli, R. D.; Lester, G. R. *Metastable Ions*; Elsevier: Amsterdam, 1973.

(28) Holmes, J. L. *Org. Mass Spectrom.* **1985**, *20*, 169–183.

(29) Wu, Z.; Fenselau, C. *J. Am. Soc. Mass Spectrom.* **1992**, *3*, 863–866.

(30) Zhang, K.; Zimmerman, D. M.; Chung-Phillips, A.; Cassady, C. J. *J. Am. Chem. Soc.* **1993**, *115*, 10812–10822.

(31) (a) Meot-Ner, M.; Hunter, E. P.; Field, F. H. *J. Am. Chem. Soc.* **1979**, *101*, 686–689. (b) Locke, M. J.; McIver, R. T. *J. Am. Chem. Soc.* **1983**, *105*, 4226–4232. (c) Gorman, G. S.; Speir, J. P.; Turner, C. A.; Amster, I. J. *J. Am. Chem. Soc.* **1992**, *114*, 3986–3988. (d) Wu, J.; Lebrilla, C. B. *J. Am. Chem. Soc.* **1993**, *115*, 3270–3275.

neglected.^{22,25,31c,32,33} This situation is encountered when chemically similar reference bases do not exist and the heterodimers are prepared with molecules from different chemical classes.

If entropy effects are not negligible, $-\Delta(\Delta S^\circ_{M^+})/R$ must be added back to eq 6, giving rise to relationship 7.

$$\ln(k/k_i) = [\Delta H^\circ_{M^+}(\text{NB})/RT_{\text{eff}} - \Delta(\Delta S^\circ_{M^+})/R] - \Delta H^\circ_{M^+}(\text{B}_i)/RT_{\text{eff}} \quad (7)$$

$$\Delta G^{\text{app}}_{M^+}(\text{NB}) = \Delta H^\circ_{M^+}(\text{NB}) - T_{\text{eff}}\Delta(\Delta S^\circ_{M^+}) \quad (8)$$

A plot of $\ln(k/k_i)$ versus $\Delta H^\circ_{M^+}(\text{B}_i)$ will now give an apparent metal ion affinity, ΔG^{app} (eq 8). It is possible to deconvolute the entropic and enthalpic contributions in this expression by determining the rate constant ratios at two different effective temperatures.^{25,34} T_{eff} is a measure of the internal energy of $[\text{NB} + \text{B}_i]\text{M}^+$ and can be changed by collisional excitation.²³ Application of eq 7 to metastable dimer ions (MI) as well as to dimer ions that have been subjected to collisionally activated dissociation (CAD) will furnish two effective temperatures (T_{MI} and T_{CAD}) and two apparent alkali ion affinities for each nucleobase. From this information, $\Delta(\Delta S^\circ_{M^+})$, i.e. the entropy difference between channels 2a and 2b, is calculated according to eq 9,

$$\Delta(\Delta S^\circ_{M^+}) = [\Delta G^{\text{app}}(\text{NB})_{\text{MI}} - \Delta G^{\text{app}}(\text{NB})_{\text{CAD}}]/(T_{\text{CAD}} - T_{\text{MI}}) \quad (9)$$

and $\Delta H^\circ_{M^+}(\text{NB})$, i.e. the alkali metal ion affinity of the nucleobase under question, from eq 8.

The described approach assumes that $\Delta(\Delta S^\circ_{M^+})$ does not depend on T_{eff} and that it remains the same for the reference bases used with a specific nucleobase. The latter should be valid if B_i are chemically similar with each other, coordinating M^+ in an analogous mode; they still may differ structurally from NB, which is not permitted by the simpler kinetic correlation of eq 6. The present paper shows that appraising $\Delta(\Delta S^\circ_{M^+})$ not only yields better $\text{NB}-\text{M}^+$ bond energy values but also reveals new insight on the structures of both $[\text{NB} + \text{B}_i]\text{M}^+$ and $[\text{NB}]\text{M}^+$.

Experimental Section

The experiments were performed with a modified VG Autospec tandem mass spectrometer of $E_1\text{BE}_2$ geometry.³⁵ Metal ion-bound dimers $[\text{NB} + \text{B}_i]\text{M}^+$ and $[\text{NB}_1 + \text{NB}_2]\text{M}^+$ were generated by FAB using ~ 12 keV Cs^+ ions as bombarding particles. Glycerol or a 5:1 mixture of dithiothreitol and dithioerythritol ("magic bullet") served as matrices. The dimer precursor ion of interest was accelerated to 8 keV, mass selected by MS-1 ($E_1\text{B}$), and allowed to dissociate spontaneously or by collision in the field free region between the magnet and the second electric sector (FFR-3). The fragments formed this way were dispersed by MS-2 (E_2) and recorded in the corresponding metastable ion (MI) or collisionally activated dissociation (CAD) mass spectrum, respectively. For CAD, He was introduced in one of the two collision cells situated in FFR-3 until the precursor ion beam was attenuated by 10%. The MI and CAD spectra measured are multiscan summations and reproducible to $\pm 5\%$. Kinetic energy releases of MI

(32) Bliznyuk, A. A.; Schaefer, H. H., III; Amster, I. J. *J. Am. Chem. Soc.* **1993**, *115*, 5149–5154.

(33) Wu, Z.; Fenselau, C. *Rapid Commun. Mass Spectrom.* **1994**, *8*, 777–780.

(34) Note that T_{eff} is not a true thermodynamic temperature because the dissociating dimer ions are not in thermal equilibrium. It should rather be viewed as a proportionality constant. See: Bojesen, G.; Breindahl, T. *J. Chem. Soc., Perkin Trans. 2* **1994**, 1029–1037. For a more recent definition of T_{eff} see: Vékey, K. *Org. Mass Spectrom.* **1996**, *31*, 445–463.

(35) Polce, M. J.; Cordero, M. M.; Wesdemiotis, C.; Bott, P. A. *Int. J. Mass Spectrom. Ion Processes* **1992**, *113*, 35–58.

Scheme 1

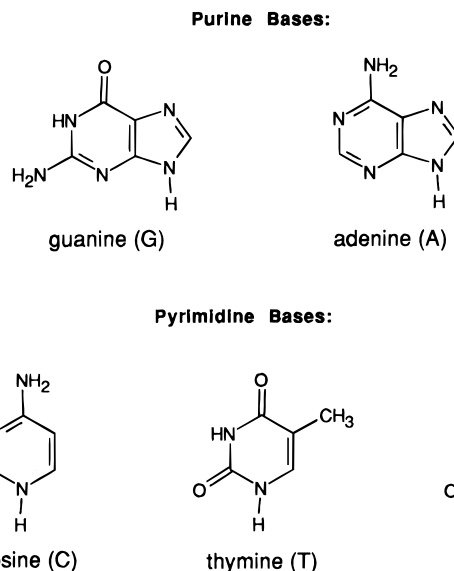


Table 1. Alkali Metal Ion Affinities of Reference Bases

	base	$\Delta H^\circ_{M^+}(\text{B}_i)$, kJ mol ⁻¹	ref
Li ⁺	glycine (Gly)	213	21
	alanine (Ala)	220	21
	valine (Val)	229	21
Na ⁺	glycine (Gly)	159	21
	alanine (Ala)	165	21
	valine (Val)	172	21
K ⁺	pyridine (Py)	86.6	36
	<i>n</i> -propylamine (Pr)	91.2	36
	aniline (An)	95.4	36

signals were calculated from peak widths at half-height ($T_{0.5}$) using established procedures.^{27,28}

The samples were prepared from saturated solutions (in the matrix) of the appropriate nucleobase, reference base, and alkali metal salt. To generate the desired heterodimer ion, 0.5-mL aliquots of the individual stock solutions were mixed and a few microliters of the resulting mixture were transferred onto the FAB probe tip. This procedure maximized the intensity of $[\text{NB} + \text{B}_i]\text{M}^+$ and $[\text{NB}_1 + \text{NB}_2]\text{M}^+$. The abundance of these adducts in the FAB spectrum was approximately 1–5% of the base peak (usually metalated or protonated matrix ions). All substances were purchased from Sigma and were used without any modification.

Results and Discussion

The Li⁺, Na⁺, and K⁺ affinities of the main DNA and RNA nucleobases (Scheme 1) were first determined based on the dissociations of $[\text{NB} + \text{B}_i]\text{M}^+$ ions, where B_i represents a reference base of known affinity. Due to the limited availability of appropriate reference molecules, *two different* series of reference bases had to be selected. With a given metal ion, the same series was used for all five nucleobases, as listed in Table 1.^{21,36} The members of each set are chemically similar, i.e. they offer the same type of bonding to M^+ . Specifically, pyridine (Py), *n*-propylamine (Pr), and aniline (An), which were used for K⁺, are unidentate ligands binding M^+ through their nitrogen lone pairs.³⁶ Glycine (Gly), alanine (Ala), and valine (Val), which were used for Li⁺ and Na⁺,²¹ are bidentate ligands coordinating M^+ between their amino and carbonyl substituents (*vide infra*).³⁷ The affinity order derived based on these B_i sets

(36) Davidson, W. R.; Kebarle, P. *J. Am. Chem. Soc.* **1976**, *98*, 6133–6138.

(37) Bouchonnet, S.; Hoppilliard, Y. *Org. Mass Spectrom.* **1992**, *27*, 71–76.

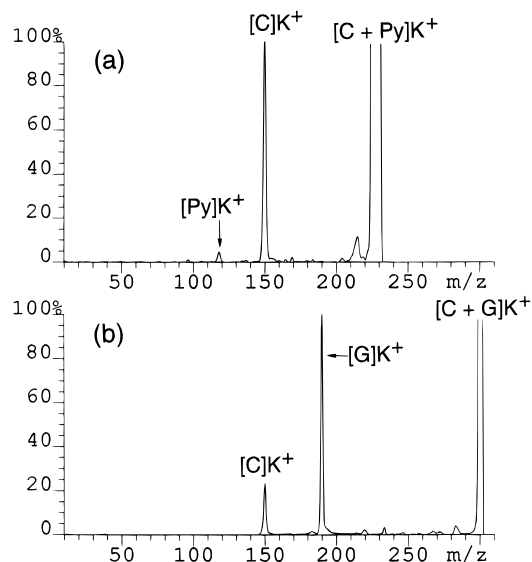


Figure 1. MI spectra of potassium-bound heterodimers containing cytosine (C) and pyridine (Py) or guanine (G). (a) [C + Py]K⁺ and (b) [C + G]K⁺.

was then validated by comparing the nucleobases with each other, i.e. by assessing the dissociations of heterodimers [NB₁ + NB₂]M⁺.

Unimolecular Reactivity of M⁺-Bridged Heterodimers.

The predominant fragments in the MI spectra of [NB + B_i]M⁺ and [NB₁ + NB₂]M⁺ are the metalated monomers [NB]M⁺ and/or [B_i]M⁺, generated according to eq 2. This is illustrated in Figure 1 for two possible combinations, namely [C + Py]K⁺ and [C + G]K⁺. The shapes of all [NB]M⁺ and [B_i]M⁺ peaks are Gaussian and the corresponding kinetic energy releases (*T*_{0.5}) about 20 meV or less. These characteristics are consistent with direct cleavages without appreciable reverse activation energy,^{27,28} as required in applications of the kinetic method (*vide supra*). The NB–M⁺ and B_i–M⁺ bonds are of electrostatic nature.¹ Hence, the reactions of eq 2 involve simple electrostatic bond dissociations, which commonly proceed with no reverse activation energy,^{12,14–16} in accord with our experimental observations.

The competitive eliminations of one NB and/or B_i unit (eq 2) remain as the principal decomposition channel also after collisional activation, as documented in Figure 2 by the CAD spectra of heterodimers [C + Val]Li⁺ and [C + G]Na⁺. No other significant fragmentation takes place, substantiating that the two bases in the dimers are weakly bridged by the central metal ion, viz. NB–M⁺–B or NB₁–M⁺–NB₂. Such a connectivity is another prerequisite that must be fulfilled before using the kinetic method to quantitatively assess NB–M⁺ bond energies (*vide supra*).

The Alkali Metal Ion Affinities of Nucleobases. The nucleobases were compared against the reference bases under both MI and CAD conditions. Each [NB + B_i]M⁺ set includes three MS/MS spectra per effective temperature, metal ion, and nucleobase, which were replicated 3–5 times. An MI spectrum from the series [C + B_i]K⁺ is shown in Figure 1a; the [C]K⁺ and [Py]K⁺ abundances in this figure indicate that the potassium ion affinity of cytosine must be larger than Δ*H*^o_{K⁺}(Py), cf. Table 1. A plot of the ln(*k*/*k*_i) values from the MI spectra of [C + B_i]K⁺ versus Δ*H*^o_{K⁺}(B_i) affords a regression line (cf. eq 7 and Figure 3) whose slope and intercept render the effective temperature of the dimers (i.e. *T*_{MI} of [C + B_i]K⁺) and the apparent K⁺ affinity of cytosine (i.e. Δ*G*^{app}_{K⁺}(C)_{MI}), respectively. Similar treatment of the CAD dissociations of [C + B_i]K⁺ supplies *T*_{CAD} and Δ*G*^{app}_{K⁺}(C)_{CAD} (Figure 3). This

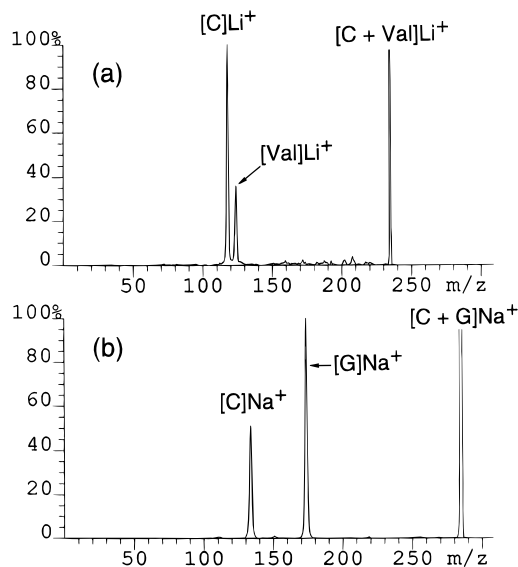


Figure 2. CAD spectra of alkali metal ion-bound heterodimers containing cytosine (C) and valine (Val) or guanine (G). (a) [C + Val]Li⁺ and (b) [C + G]Na⁺.

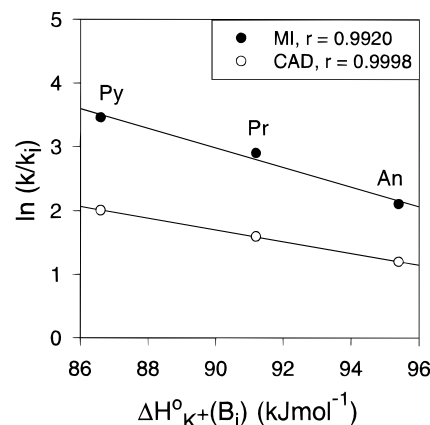


Figure 3. Plot of ln(*k*/*k*_i) versus Δ*H*^o_{K⁺}(B_i) at two effective temperatures for [C + B_i]K⁺ dimers containing cytosine and the reference base (B_i) aniline (An), *n*-propylamine (Pr), or pyridine (Py). The rate constant ratio *k*/*k*_i is calculated by dividing the abundances of [C]K⁺ and [B_i]K⁺ in the corresponding MI (filled circles) or CAD spectra (open circles). The slopes of these lines provide the effective temperatures (*T*_{MI} and *T*_{CAD}, respectively), while their intercepts provide the corresponding apparent potassium ion affinities of cytosine.

Table 2. Li⁺ Affinities of the Nucleobases Based on the Dissociation of [NB + B_i]Li⁺ Dimers

nucleobase	Δ <i>G</i> ^{app} _{MI} , kJ mol ⁻¹	<i>T</i> _{MI} , K	Δ <i>G</i> ^{app} _{CAD} , kJ mol ⁻¹	<i>T</i> _{CAD} , K	Δ(Δ <i>S</i> ^o _{Li⁺}), J mol ⁻¹ K ⁻¹	Δ <i>H</i> ^o _{Li⁺} , kJ mol ⁻¹
guanine (G)	242	819	245	1517	-4.3	239
cytosine (C)	235	736	238	1506	-3.9	232
adenine (A)	230	712	234	1495	-5.1	226
thymine (T)	225	884	231	1439	-10.8	215
uracil (U)	225	970	230	1330	-13.9	211

information and eqs 8 and 9 allow one to calculate the K⁺ affinity of cytosine, Δ*H*^o_{K⁺}(C), as well as the difference in bond dissociation entropies between the C–K⁺ and B_i–K⁺ bonds, Δ(Δ*S*^o_{K⁺}). Tables 2–4 summarize the Li⁺, Na⁺, and K⁺ affinities of the five nucleobases resulting using this procedure, along with the corresponding Δ(Δ*S*^o) values. The error limits in these data are ±4 kJ mol⁻¹ and ±1.5 J mol⁻¹ K⁻¹, respectively, and primarily reflect the uncertainty in Δ*H*^o_{M⁺} of the reference bases (Table 1); the accuracy of relative alkali metal ion affinities, i.e. of Δ(Δ*H*^o_{M⁺}) between individual nucleobases, is better than ±2 kJ mol⁻¹. The nucleobase

Table 3. Na⁺ Affinities of the Nucleobases Based on the Dissociation of [NB + B_i]Na⁺ Dimers

nucleobase	$\Delta G_{\text{MI}}^{\text{app}}$, kJ mol ⁻¹	T_{MI} , K	$\Delta G_{\text{CAD}}^{\text{app}}$, kJ mol ⁻¹	T_{CAD} , K	$\Delta(\Delta S_{\text{Na}^+}^{\circ})$, J mol ⁻¹ K ⁻¹	$\Delta H_{\text{Na}^+}^{\circ}$, kJ mol ⁻¹
guanine (G)	186	645	190	1246	-6.7	182
cytosine (C)	181	535	190	1763	-7.3	177
adenine (A)	178	787	183	1407	-8.1	172
thymine (T)	157	910	161	1199	-13.8	144
uracil (U)	152	904	164	1909	-11.9	141

Table 4. K⁺ Affinities of the Nucleobases Based on the Dissociation of [NB + B_i]K⁺ Dimers

nucleobase	$\Delta G_{\text{MI}}^{\text{app}}$, kJ mol ⁻¹	T_{MI} , K	$\Delta G_{\text{CAD}}^{\text{app}}$, kJ mol ⁻¹	T_{CAD} , K	$\Delta(\Delta S_{\text{K}^+}^{\circ})$, J mol ⁻¹ K ⁻¹	$\Delta H_{\text{K}^+}^{\circ}$, kJ mol ⁻¹
guanine (G)	112	663	106	1529	+6.9	117
cytosine (C)	106	620	102	1258	+6.3	110
adenine (A)	101	724	98	1160	+6.9	106
thymine (T)	101	445	100	885	+2.3	102
uracil (U)	100	518	99	1039	+1.9	101

affinities measured in this study (Tables 2–4) are in very good agreement with $\Delta H_{\text{M}^+}^{\circ}$ values from threshold CAD measurements reported recently by Rodgers and Armentrout.¹²

It is noticed in Tables 2–4 that the effective temperatures T_{MI} and (especially) T_{CAD} change for the different nucleobases. T_{MI} and T_{CAD} reflect the internal energies of the metastable and collisionally activated [NB + B_i]M⁺ ions, respectively (*vide supra*). They depend on several factors, including sample preparation, internal energy distribution upon ionization, the nucleobase structure, and (T_{CAD}) the collisional cross-sections of the dimer ions with the target used for CAD. Even under constant experimental conditions, some of these variables cannot be controlled and could cause the observed fluctuations.

With all three metal ions studied, the affinities increase in the order uracil < thymine < adenine < cytosine < guanine. It is noteworthy that the proton affinities of the DNA nucleobases rise in the same direction,¹³ suggesting that a higher basicity also incurs stronger bonding to alkali metal ions. The NB–M⁺ bond energies decrease as the size of the metal ion becomes larger. Such a trend has already been observed for other types of ligands.^{21,37}

The difference in a specific metal ion affinity between two nucleobases (relative affinity) often is only a few kJ mol⁻¹, i.e. very close to the experimental error limit (*vide supra*). For this reason, we cross-checked the derived affinity orders by examining the behavior of heterodimers [NB₁ + NB₂]M⁺, in which one nucleobase is used as the unknown (NB₁) and 2–3 of the other as reference (NB₂). Figures 1b and 2b give examples of MI and CAD spectra, respectively, while Figure 4 illustrates representative $\ln(k_1/k_2)$ plots for dimers composed of thymine and another nucleobase, viz. [T + NB₂]Na⁺. The $\Delta H_{\text{M}^+}^{\circ}(\text{NB})$ values resulting from such experiments are presented in Table 5 and generally agree well with those obtained using the reference bases. For all three alkali metal ions, the order of NB–M⁺ bond strengths remains unchanged; guanine stands out showing the highest affinity, followed by cytosine > adenine > thymine > uracil. The two latter nucleobases are the poorest ligands and just distinguishable from each other. It is of interest to note in this context, that thymine and uracil perform analogous functions *in vivo* (pairing with adenine), the former in DNA and the latter in RNA.

Inspection of Tables 2–4 shows that neglecting entropy effects would have led to conflicting orders. For example, the apparent potassium ion affinity of adenine ($\Delta G_{\text{K}^+}^{\text{app}}$) is equal to that of thymine under MI but lower than thymine's under CAD conditions. After accounting for the corresponding

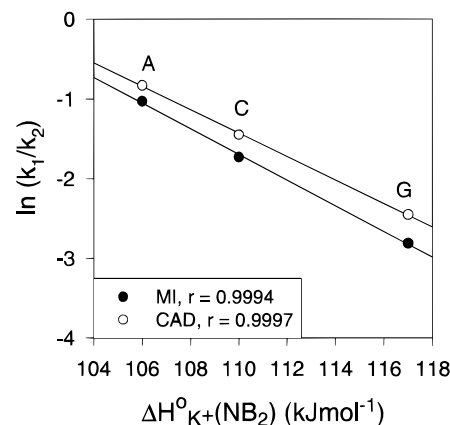


Figure 4. Plot of $\ln(k_1/k_2)$ versus $\Delta H_{\text{K}^+}^{\circ}(\text{NB}_2)$ for [NB₁ + NB₂]K⁺ dimers at two effective temperatures; NB₁ is thymine (T) and NB₂ is guanine (G), cytosine (C), or adenine (A). The rate constant ratio k_1/k_2 is calculated by dividing the abundances of [T]K⁺ and [NB₂]K⁺ in the corresponding MI (filled circles) or CAD spectra (open circles).

$\Delta(\Delta S_{\text{K}^+}^{\circ})$ term, cf. Table 4, the correct ranking of adenine and its real K⁺ affinity ($\Delta H_{\text{K}^+}^{\circ}$) are obtained. The $\Delta(\Delta S_{\text{M}^+}^{\circ})$ values measured further indicate that, had entropy effects not been considered, the K⁺ affinities of the nucleobases would have been underestimated while their Li⁺ and Na⁺ affinities would have been overestimated.

It is evident from Tables 2–5 that the entropic contributions, viz. $T_{\text{eff}}\Delta(\Delta S_{\text{M}^+}^{\circ})$, are small compared to the apparent affinity values; they are, however, similar to the difference in affinity between nucleobases, i.e. to $\Delta(\Delta G_{\text{M}^+}^{\text{app}})$ or $\Delta(\Delta H_{\text{M}^+}^{\circ})$. Hence, $\Delta(\Delta S_{\text{M}^+}^{\circ})$ can obscure the affinity ranking of certain nucleobases and must be taken into account for assessing the correct order of NB–M⁺ bond enthalpies. The value of $\Delta(\Delta S_{\text{M}^+}^{\circ})$ depends on the nucleobase, the reference bases, and (to a lesser degree) the metal ion. As discussed in the following section, the $\Delta(\Delta S_{\text{M}^+}^{\circ})$ dependence on these variables provides information about how the metal ion is coordinated in both the heterodimer and its dissociation products.

Entropy Considerations. The apparent metal ion affinities obtained under MI and CAD conditions differ from each other (Table 2–4), indicating that the entropy changes associated with the competing dissociations 2a and 2b do not cancel. The net change, i.e. $\Delta(\Delta S_{\text{M}^+}^{\circ}) = \Delta S_{\text{M}^+}^{\circ}(\text{NB}) - \Delta S_{\text{M}^+}^{\circ}(\text{B}_i)$, is either positive or negative and its magnitude varies for each nucleobase within a set of reference bases, pointing to a possible relationship between the entropy term $\Delta(\Delta S_{\text{M}^+}^{\circ})$ and the nucleobase structure.

$\Delta(\Delta S_{\text{M}^+}^{\circ})$ encompasses translational, vibrational, and rotational contributions.^{38,39} For ligand exchange reactions involving Li⁺ and simple Lewis bases (i.e. B₁Li⁺ + B₂ → B₁ + B₂Li⁺), Beauchamp et al. showed that the overall change in rotational entropy is more significant than changes in either translational or vibrational entropies.³⁹ Arguments can be made that an analogous situation pertains to the decompositions of a metal-bound dimer into the corresponding metalated monomers, viz. eq 2. The net translational entropy change is expected to be minimal, because the increase in the number of translational degrees of freedom is similar for eqs 2a and 2b. Due to the common character of the bonds being broken in these two pathways (both of electrostatic nature),^{36,39} the vibrational portion of $\Delta(\Delta S_{\text{M}^+}^{\circ})$ should also be quite small, leaving rotational entropy as the major contributor to $\Delta(\Delta S_{\text{M}^+}^{\circ})$. Being

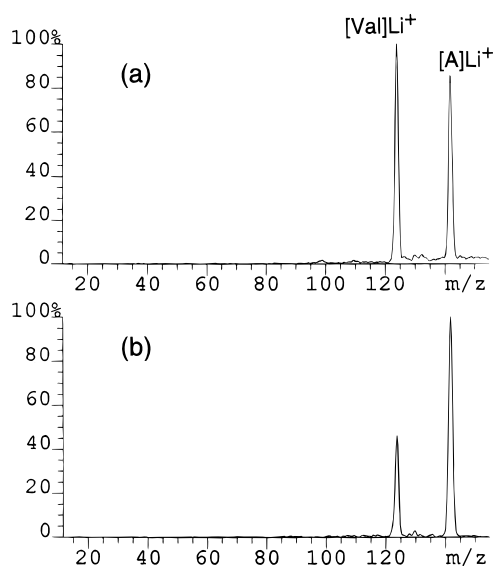
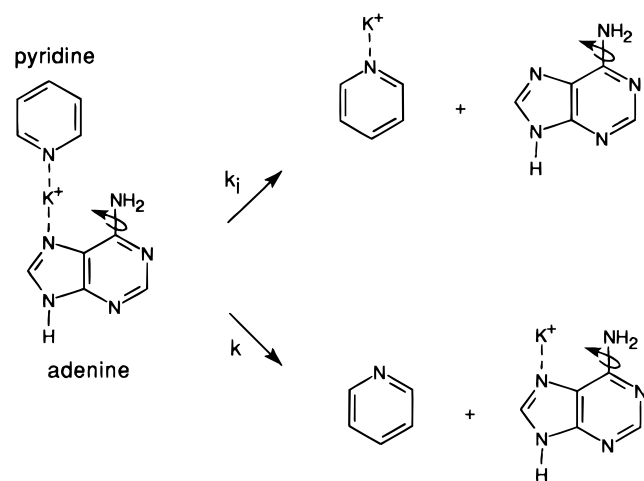
(38) Searles, S. K.; Kebarle, P. *Can J. Chem.* **1969**, *47*, 2619–2627.

(39) Woodin, R. L.; Beauchamp, J. L. *J. Am. Chem. Soc.* **1978**, *100*, 501–508.

Table 5. Alkali Ion Affinities of the Nucleobases Based on the Dissociation of [NB₁ + NB₂]M⁺ Dimers (M⁺ = Li⁺, Na⁺, K⁺)

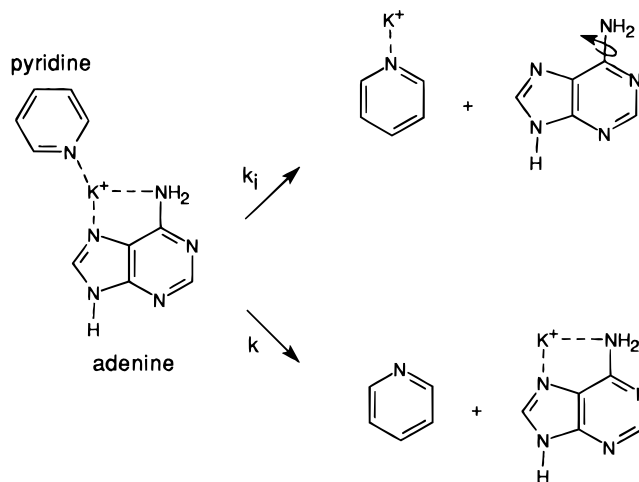
nucleobase NB ₁	ref bases NB ₂ ^b	$\Delta H_{\text{Li}^+}^\circ$, kJ mol ⁻¹	$\Delta(\Delta S_{\text{Li}^+}^\circ)^a$, J mol ⁻¹ K ⁻¹	$\Delta H_{\text{Na}^+}^\circ$, kJ mol ⁻¹	$\Delta(\Delta S_{\text{Na}^+}^\circ)^a$, J mol ⁻¹ K ⁻¹	$\Delta H_{\text{K}^+}^\circ$, kJ mol ⁻¹	$\Delta(\Delta S_{\text{K}^+}^\circ)^a$, J mol ⁻¹ K ⁻¹
guanine (G)	C, A	239	0.0	185	-0.3	114	+0.7
	T, U	237	+8.0	187	+11.0	114	+12.7
cytosine (C)	G, A	231	+0.5	175	-0.7	111	-0.2
	T, U	233	+6.0	173	+9.0	111	+10.0
adenine (A)	G, C	227	-0.9	172	-1.0	107	-0.3
	T, U	226	+6.0	174	+10.0	109	+11.0
thymine (T) ^c	G, C, A	213	-9.0	148	-14.8	94	-8.0
uracil (U) ^c	G, C, A	211	-9.8	138	-15.0	93	-9.0

^a $\pm < 3$ J mol⁻¹ K⁻¹. ^b See discussion of entropy effects for the criteria of reference base selection. ^c From the dimer [T + U]M⁺, in which thymine and uracil are compared directly to each other, [T]M⁺ is produced with a higher relative abundance than [U]M⁺ both under MI and CAD conditions.

**Figure 5.** (a) MI spectrum and (b) CAD spectrum of the Li⁺-bound heterodimer containing adenine and valine, viz. [A + Val]Li⁺.**Scheme 2**

multifunctional molecules, nucleobases (and some of the reference bases used) allow chelation, which can restrict rotations and, thereby, bring upon substantial entropy effects (*vide infra*).

Nucleobase-Controlled Entropy Effects in [NB + B_i]K⁺ Dimers. Scheme 2 shows the dissociation of an “idealized” K⁺-bound dimer, composed of pyridine and adenine, in which the simplified form of the kinetic method could be used. In this case, the binding of K⁺ to pyridine or adenine in both the dimer as well as the monomers does not significantly affect rotational degrees of freedom in either of these species and, therefore, $\Delta(\Delta S_{\text{K}^+}^\circ)$ should be near zero. However, the $\Delta(\Delta S_{\text{K}^+}^\circ)$

Scheme 3

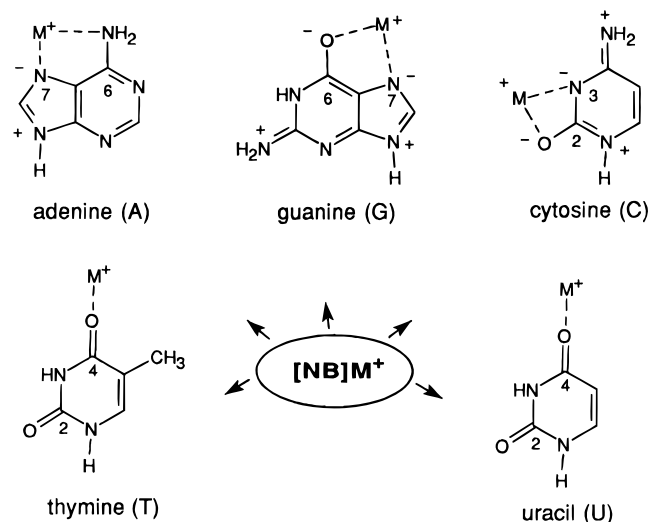
value actually obtained (+6.9 J mol⁻¹ K⁻¹, cf. Table 4) does not support such a simple mechanism. Scheme 2 shows K⁺ attached in a *unidentate* fashion to the N-7 position of adenine, which is a favored metalation site in solution.⁴⁰ Likewise, *unidentate* attachment to any other site of adenine does not prohibit any rotations and would be inconsistent with the measured entropy change.

The reference bases used for the K⁺ affinities (pyridine, *n*-propylamine, and aniline) are unable to complex the metal ion in a multidentate fashion. In contrast, chelation is possible with adenine, cf. Scheme 3, and would freeze the rotations of its amino group, which in turn can explain the observed $\Delta(\Delta S_{\text{M}^+}^\circ)$. From dimer [Py + A]K⁺, the formation of [Py]K⁺ + A is associated with a more positive entropy change than the formation of Py + [A]K⁺, because adenine recovers the NH₂ rotations once released from the K⁺-bound dimer; overall, $\Delta(\Delta S_{\text{K}^+}^\circ)$ increases. This favorable entropy change enhances the abundance of [Py]K⁺, making the potassium ion affinity of adenine appear somewhat closer to that of pyridine than it really is: compare adenine's $\Delta G_{\text{K}^+}^{\text{app}}$ and $\Delta H_{\text{K}^+}^\circ$ entries in Table 4 to $\Delta H_{\text{K}^+}^\circ(\text{Py})$ in Table 1. Entropic effects become more pronounced at a higher effective temperature (see eq 8). Indeed, the discrepancy between $\Delta G_{\text{K}^+}^{\text{app}}$ and $\Delta H_{\text{K}^+}^\circ$ of adenine increases from MI to CAD (Table 4).⁴¹

Based on the forgoing discussion, the entropy parameter associated with the dissociation of [Py + A]K⁺ strongly suggests that the amino substituent is involved in the bonding of adenine to potassium ion. In solution, this group and N-7 form bidentate complexes to metal ions.⁴⁰ K⁺ attachment between these sites, as shown in Scheme 3, is in keeping with our findings. Recent

(40) Marzilli, L. G.; Kistenmacher, T. J.; Eichhorn, G. L. In *Nucleic Acid-Metal Ion Interactions*; Spiro, T. G., Ed.; John Wiley & Sons: New York, 1980; pp 179–250.

Scheme 4

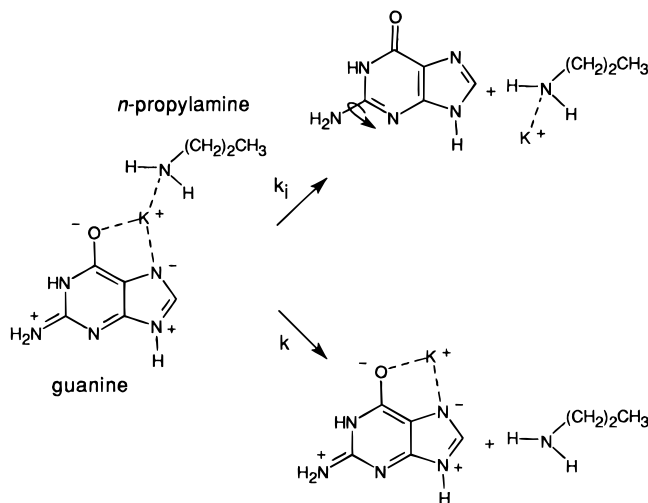


theoretical calculations by Rodgers and Armentrout have predicted a similar coordination in lithiated adenine,¹² supporting our proposition in Scheme 3. The nucleobases are highly conjugated systems with several resonance forms. It is therefore conceivable that the chelate between adenine and K^+ (or the other alkali metal ions, see below) is stabilized by the formation of an ion pair (i.e. a salt bridge), as rationalized in Scheme 4.⁴²

An alternative scenario would be that the $[Py + A]K^+$ dimer has the structure shown in Scheme 2 and dissociates to yield the chelated $[A]K^+$ product shown in Scheme 3. This reaction channel demands a tighter transition state and should be associated with a considerable reverse activation energy and kinetic energy release compared to the competing formation of $[Py]K^+$. The $T_{0.5}$ values for $[A]K^+$ and $[Py]K^+$ from metastable $[Py + A]K^+$ are however similar and relatively small (~ 20 meV, *vide supra*) and do not support such a mechanism.^{27,28} Moreover, formation of $[A]K^+$ via a tight transition state would slow down this process, essentially making it noncompetitive against the formation of $[Py]K^+$ via a loose transition state.²⁷

According to Table 4, the $\Delta(\Delta S^\circ_{K^+})$ values for guanine and cytosine are comparable to that of adenine in both sign and magnitude. Evidently, the amino groups in G and C participate, too, in the complexation of the metal ion. Likely chelates in which the NH_2 rotor is blocked are included in Scheme 4. In the proposed structures, M^+ attaches at N-7 and C=O-6 in guanine and at N-3 and C=O-2 in cytosine; these are the metalation locations predicted by theory¹² and favored in solution.⁴⁰ Note that the amino functionality is not directly involved in the bonding, but can still lose its rotational flexibility through ion pair formation, which creates doubly-bonded (and hence rotationally restricted) immonium ions.^{43,44} As rationalized in Scheme 5 for heterodimer $[Pr + G]K^+$, the lost rotational degrees of freedom are recovered when the nucleobase detaches from the metal ion. The resulting entropy gain causes the K^+

Scheme 5



affinities of guanine and cytosine to appear smaller than they are (cf. ΔG^{app} vis à vis ΔH° in Table 4).

Thymine and uracil have the smallest $\Delta(\Delta S^\circ_{K^+})$ values. This is not surprising, as both these bases possess no free rotors that could interact with the metal ion. In solution, metal ions bind at one of the carbonyl groups;⁴⁰ this could also be true in the gas phase. The structures in Scheme 4 have M^+ attached to C=O-4, the preferred site of attachment indicated by theory.¹²

Reference Base-Controlled Entropy Effects in $[NB + B_i]Li^+$ and $[NB + B_i]Na^+$ Dimers. With the K^+ -bound dimers discussed above, $\Delta(\Delta S^\circ_{M^+})$ originates essentially upon cleaving the $NB-K^+$ bond; the B_i-K^+ bond cleavages do not contribute appreciably to the net entropy change. This scenario documents itself by a decrease in the nucleobase's apparent metal ion affinity as the effective temperature increases, which then leads to positive $\Delta(\Delta S^\circ_{M^+})$ values (cf. eq 9 and Table 4). With Li^+ and Na^+ the opposite is true (Tables 2 and 3), pointing out that the reference bases B_i used for these metal ions (i.e. Gly, Ala, Val) cause larger entropy changes than the nucleobases.

Theoretical studies by Bouchonnet and Hoppilliard on the structure of sodiated glycine have shown that the most stable form of $[Gly]Na^+$ arises by coordination of the metal cation between the carbonyl oxygen and the amino group.³⁷ A similar binding mode is expected for $[Gly]Li^+$ as well as for the Na^+ and Li^+ adducts of Ala and Val. Such metal ion complexation hinders rotations around the H_2N-C^α and $C^\alpha-CO$ bonds of the amino acids, as depicted in Scheme 6 for the dissociating heterodimer $[Gly + A]Li^+$. In this example, binding to lithium restricts more rotations in the amino acid than in the nucleobase. As a consequence, there is less entropy gain upon the formation of $[Gly]Li^+ + A$ than upon the formation of $Gly + [A]Li^+$, resulting in a negative $\Delta(\Delta S^\circ_{Li^+})$ quantity. A net entropy loss would increase the apparent Li^+ affinity of adenine upon CAD (eq 9), which is true (Table 2). Parallel observations are made for the apparent Na^+ affinity and $\Delta(\Delta S^\circ_{Na^+})$ term of adenine (Table 3), confirming that Li^+ and Na^+ bind alike to the amino acid reference bases B_i and to adenine.

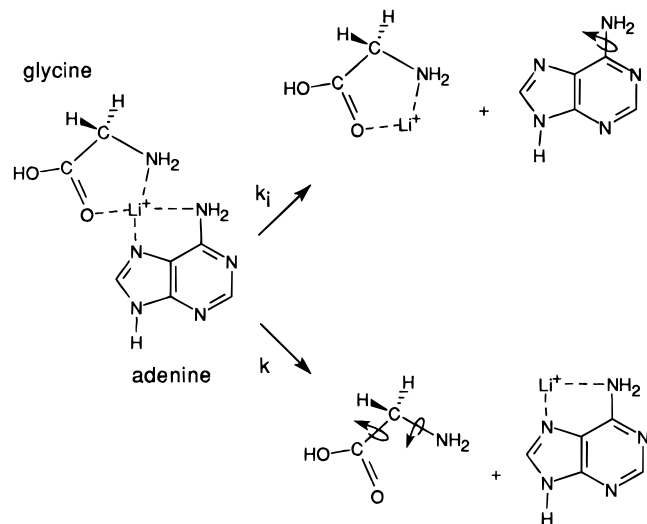
(41) The entropy changes described in Scheme 3 evolve in the respective transition states which affect the dissociation kinetics and product ion abundances. The transition state leading to $[Py]K^+ + A$ can be envisioned as having elongated bonds between K^+ and A, allowing for some rotational flexibility in the NH_2 substituent; on the other hand, that leading to $Py + [A]K^+$ will have a stretched $Py-K^+$ bond, but the K^+ coordination to A (and, hence, the rotational restriction of NH_2) still intact. Note that, because the metalated monomers are formed in endothermic dissociations with no reverse activation energy, the corresponding transition states rather resemble the separated products than the precursor ion.^{27,28} Parallel arguments apply to Schemes 5 and 6 (*vide infra*).

(42) Campbell, S.; Rodgers, M. T.; Marzluff, E. M.; Beauchamp, J. L. *J. Am. Chem. Soc.* **1995**, *117*, 12840–12854.

(43) Rotation around the $C-NH_2$ bond of cytosine would also be hindered if the metal ion attaches between the amino group and N-3. Such a chelation does not take place in solution;⁴⁰ moreover, it only allows for one ion pair with M^+ (in a four-membered-ring setting), which would not explain the higher $\Delta H^\circ_{M^+}$ values of cytosine vis à vis adenine. Parallel arguments speak against coordination of M^+ near the amino group of guanine.

(44) A small part of the entropy change for adenine, cytosine, and guanine could originate from restriction of the wagging vibrations of the exocyclic substituents that coordinate M^+ ; Rodgers, M. T., private communication.

Scheme 6



The $\Delta(\Delta S^\circ_{\text{Li}^+})$ and $\Delta(\Delta S^\circ_{\text{Na}^+})$ values of guanine and cytosine also are negative and fairly similar to those of adenine (Tables 2 and 3), in keeping with the presence in these three nucleobases of an amino rotor that can freeze upon attachment of the metal ion (Scheme 4).⁴⁴ On the other hand, thymine and uracil show much larger net entropy losses (Tables 2 and 3). These latter nucleobases recover no rotational degrees of freedom after losing the metal ion. Now, a minor change in rotational entropy upon fragmentation to $[\text{B}_i]\text{M}^+ + \text{T}$ or U is accompanied by a much larger change upon fragmentation to $\text{B}_i + [\text{T}$ or $\text{U}]\text{M}^+$, thus giving rise to an overall more negative $\Delta(\Delta S^\circ_{\text{M}^+})$ amount.

Significant entropy effects may obstruct abundance ratios in MI and CAD spectra, leading to contradicting conclusions about relative affinities. This is demonstrated for the heterodimer $[\text{Val} + \text{A}]\text{Li}^+$ in Figure 5, where the MI spectrum implies that valine has a higher Li^+ affinity than adenine, while the CAD spectrum predicts the reverse order. In reality, the $\text{Val}-\text{Li}^+$ bond is stronger than the $\text{A}-\text{Li}^+$ bond (compare $\Delta H^\circ_{\text{M}^+}$ values in Tables 1 and 2), but the formation of $[\text{Val}]\text{Li}^+ + \text{A}$ is discriminated against entropically (cf. Scheme 6), which enhances the apparent lithium ion affinity of adenine. This entropic enhancement is most severe upon CAD (i.e. at the higher effective temperature), now causing an inversion of the abundance ratio of the $[\text{Val}]\text{Li}^+$ and $[\text{A}]\text{Li}^+$ fragments. Grützmacher and Caltapanides have reported similar inversions upon the dissociation of proton-bound dimers.⁴⁵

Irrespective of the metal ion involved, the net entropy changes for guanine, cytosine, and adenine are comparable to but different from those of thymine and uracil. With all three metal ions, the observed entropy effects can be rationalized by the structures of Scheme 4, in which the amino groups of the three NH_2 bearing nucleobases are involved in the coordination of the metal ion either directly (A) or through resonance (G and C). T and U, which lack this electron-donating substituent, form the weakest bonds to all three alkali metal ions. For a given nucleobase the $\Delta(\Delta S^\circ_{\text{Li}^+})$ and $\Delta(\Delta S^\circ_{\text{Na}^+})$ terms, which result from the *same set* of reference bases, show equivalent signs and magnitudes (cf. Tables 2 and 3). This reinforces our above proposition that, independent of the nature of the alkali metal ion, the metalated monomers and dimers of a given nucleobase possess equivalent structures. It is also worth noting that the attachment sites shown in Scheme 4 agree well with the optimized structures of $[\text{NB}]\text{Li}^+$ derived theoretically by Rodgers and Armentrout.¹²

(45) Grützmacher, H.-F.; Caltapanides, A. *J. Am. Soc. Mass Spectrom.* **1994**, *5*, 826–836.

Entropy Effects in the Dissociation of $[\text{NB}_1 + \text{NB}_2]\text{M}^+$ Dimers. In the comparison of the nucleobases to each other, a specific base NB_1 was paired with a set of nucleobases (designated as NB_2) that exhibit common entropic features. Our measurements with reference bases have identified two families of NB_2 , namely NH_2 carrying adenine, cytosine, and guanine as well as rotor-free thymine and uracil. The heterodimers investigated in this manner are listed in Table 5, along with the resulting affinities and net entropy changes.

When guanine, cytosine, and adenine are compared against nucleobases from the same family, entropy effects virtually cancel out and $\Delta(\Delta S^\circ_{\text{M}^+})$ is zero or negligible. In sharp contrast, when the comparison of G, C, or A is made against thymine and uracil, which belong to a different structural class (*vide supra*), appreciable *positive* $\Delta(\Delta S^\circ_{\text{M}^+})$ values are observed in all cases. Note that a positive $\Delta(\Delta S^\circ_{\text{M}^+})$ results if the reference bases have no restrictable rotors, which applies to T and U (see their NB_2 entries in Table 5) and to the reference bases used for K^+ (Table 4). Large net entropy changes also occur when thymine and uracil act as the nucleobase of unknown affinity (NB_1) and are contrasted to reference bases G, C, and A. In these instances, however, the net $\Delta(\Delta S^\circ_{\text{M}^+})$ value is *negative*, because the reference bases endure more serious alteration of their rotational freedom (upon attachment or detachment of M^+) than either thymine or uracil; such reference-controlled entropic effects were encountered with the amino acids utilized in Li^+ and Na^+ heterodimers (cf. Tables 2 and 3 versus the last two rows in Table 5).

The sign and magnitude of the $\Delta(\Delta S^\circ_{\text{M}^+})$ term primarily depend on the nature of NB_1 and NB_2 and much less on the metal ion, corroborating that Li^+ , Na^+ , and K^+ bind very similarly to the nucleobases, as generalized in Scheme 4. The postulated structures are fully supported by the observed $\Delta(\Delta S^\circ_{\text{M}^+})$ values. They also help explain the common metal ion affinity order $\text{G} > \text{C} > \text{A} > \text{T} > \text{U}$ on the basis of the coordination sites available in these nucleobases and their ability to form ion pairs.

Ion pairs are common in the solid state (e.g., in salts) and in solution (e.g., in enzymatic reactions where the expressions *ion pair* and *salt bridge* are used as synonyms). Recent studies by Beauchamp et al.⁴² and others⁴⁶ have revealed that ion pairs are feasible in the gas phase, too (e.g., in protonated peptides⁴² or acid–base complexes⁴⁶). The captodative substitution pattern of certain nucleobases makes them capable of adopting zwitterionic structures,⁴⁷ which can then form ion pairs with the approaching electrophilic alkali metal cation. The superior M^+ affinities of guanine, cytosine, and adenine are attributed to such ion pair formation (cf. Scheme 4). The conjugate systems of guanine and cytosine can lead to salt bridges at both sites attaching to M^+ , explaining the higher bond energies of $\text{G}-\text{M}^+$ and $\text{C}-\text{M}^+$ versus that of $\text{A}-\text{M}^+$. According to studies by Castleman et al., Na^+ binds stronger to acetone than to either methylamine or methanol;⁴⁸ hence, an additional reason for the larger M^+ affinities of guanine and cytosine, compared to adenine, could be the preference of alkali metal ions for binding to carbonyl groups.²² Further, guanine can coordinate M^+ in a five-membered-ring arrangement, which is more stable than the four-membered ring resulting with cytosine (Scheme 4), justifying $\Delta H^\circ_{\text{M}^+(\text{G})} > \Delta H^\circ_{\text{M}^+(\text{C})}$. The lower affinities of thymine

(46) Legon, A. *Chem. Soc. Rev.* **1993**, *22*, 153–163.

(47) (a) Viehe, H. G.; Janousek, Z.; Merényi, R.; Stella, L. *Acc. Chem. Res.* **1985**, *18*, 148–154. (b) Sustmann, R.; Korth, H.-G. *Adv. Phys. Org. Chem.* **1990**, *26*, 131–177.

(48) Guo, B. C.; Conklin, B. J.; Castleman, A. W., Jr. *J. Am. Chem. Soc.* **1989**, *111*, 6506–6510.

and uracil could be due to the weaker interaction provided by a monodentate bonding of the metal ion (Scheme 4) and/or to a lower extent of ion pair formation in these nucleobases.⁴⁹ Finally, the ranking $T > U$ should be the consequence of inductive effects, created by the methyl group in thymine. Since inductive stabilization is exerted through σ -bonds at short distances, the carbonyl group next to CH_3 (i.e. C=O-4) would be the primary beneficiary and, hence, is the likely M^+ attachment site in thymine and uracil.

Conclusions

The modified approach of the Cooks' kinetic method presented in this study detects and evaluates the net entropy change occurring upon the dissociation of metal ion-bound heterodimers. This change is quantitatively assessed using simple MS/MS techniques and deconvoluted from experimentally measured free energies, to ultimately yield M^+ -ligand bond enthalpies (i.e. metal ion affinities). The usefulness of this approach is demonstrated by the derivation of the Li^+ , Na^+ , and K^+ affinities of the fundamental DNA and RNA nucleobases. The affinity values of individual nucleobases are found to be fairly similar; as a result, entropic corrections are essential for the determination of the correct affinity order, which is obscured if entropy is not considered.

(49) With thymine and uracil, electron donation by N-1 (or N-3) to C=O-4, to yield the ion pair $\text{=C-O}^- \text{M}^+$, generates a positive charge at N-1 (or N-3), which would be destabilized by the adjacent electron-withdrawing carbonyl group (i.e. by C=O-2). Therefore, salt bridge creation is less probable with these two nucleobases. It should be mentioned, however, that some coordination of M^+ with the lone pair of N-3 may take place resulting in a complex similar to that shown for cytosine in Scheme 4 but with a lesser tendency to form salt bridges. Such a situation would not change the data interpretation or any of the conclusions made.

A major obstacle in using the simple kinetic approach (which ignores entropy effects) is the need to use reference bases that are structurally similar to the unknown base. With multifunctional unknowns, such bases often do not exist. The method presented removes this requirement, widening the applicability of the kinetic method; *still*, the set of reference molecules must remain chemically similar.

Finally, an encouraging finding is that the analysis of entropy effects unveils novel structural insight. In the present investigation, the entropy term provided evidence for the involvement of amino rotors in the coordination of the alkali metal ion. This important information helped postulate metal ion-nucleobase binding modes that are consistent with all experimental data. Such an approach complements more classical MS/MS techniques which decipher ion structures through their fragmentation patterns; the described method is currently expanded to metalated peptides and saccharides to learn more about how metal ions are coordinated by these rotationally more flexible biomolecules.

Acknowledgment. This project was supported by the National Institutes of Health and the University of Akron. We extend our gratitude to Dr. Šárka Beranová, Dr. Kim Calvo, and Michael J. Polce for experimental assistance and motivating discussions, to Dr. Mary T. Rodgers and Dr. Peter B. Armentrout for communication of threshold CAD results, theoretical data, and helpful comments (refs 12 and 44), to Dr. R. Graham Cooks for useful suggestions about fragmentation pathways of metalated dimers, and to Dr. Stephen D. Darling for providing us with Darling model sets of the nucleobases.

JA9613421